

Importance of borehole deviation surveys for monitoring of hydraulic fracturing treatments

Petr Bulant^{1*}, Leo Eisner², Ivan Pšenčík³ and Joël Le Calvez⁴

¹Charles University in Prague, Czech Republic, ²Schlumberger Cambridge Research, UK, ³Geophysical Institute of the Academy of Sciences of the Czech Republic, Czech Republic, and ⁴Schlumberger Data Consulting Services, Houston, USA

Received November 2006, revision accepted April 2007

ABSTRACT

During seismic monitoring of hydraulic fracturing treatment, it is very common to ignore the deviations of the monitoring or treatment wells from their assumed positions. For example, a well is assumed to be perfectly vertical, but in fact, it deviates from verticality. This can lead to significant errors in the observed azimuth and other parameters of the monitored fracture-system geometry derived from microseismic event locations. For common hydraulic fracturing geometries, a 2° deviation uncertainty on the positions of the monitoring or treatment well survey can cause a more than 20° uncertainty of the inverted fracture azimuths. Furthermore, if the positions of both the injection point and the receiver array are not known accurately and the velocity model is adjusted to locate perforations on the assumed positions, several-millisecond discrepancies between measured and modeled SH-P traveltimes may appear along the receiver array. These traveltimes discrepancies may then be misinterpreted as an effect of anisotropy, and the use of such anisotropic model may lead to the mislocation of the detected fracture system. The uncertainty of the relative positions between the monitoring and treatment wells can have a cumulative, nonlinear effect on inverted fracture parameters. We show that incorporation of borehole deviation surveys allows reasonably accurate positioning of the microseismic events. In this study, we concentrate on the effects of horizontal uncertainties of receiver and perforation positions. Understanding them is sufficient for treatment of vertical wells, and also necessary for horizontal wells.

INTRODUCTION

In oil and gas production, a process known as hydraulic fracturing is often used to increase the productivity of hydrocarbon reservoirs. Hydraulic fracturing involves pumping various types of fluids under pressure down a treatment well into the reservoir. The pressurized fluid enters the reservoir and fractures the reservoir rock. These fractures increase permeability and conductivity, and ultimately production. To keep these fractures highly conductive, solid particles known as proppant are pumped with the fluid into the created fractures. Creation

of fractures and opening of pre-existing fractures generates microseismic events observed by geophones located in a monitoring borehole. The fracture geometry is then determined from locations of these events. For the sake of brevity, we are going to use the term “microseismic monitoring” throughout the paper. When using it, we keep in mind that we mean monitoring of induced microseisms generated in relation to hydraulic fracturing treatment.

Over the years, a large number of hydraulic fracturing treatments have been monitored to determine fracture geometries (e.g., Warpinski *et al.* 1998; Rutledge and Phillips 2003; Berumen *et al.* 2004). Usually, only a single (very often, the closest) monitoring borehole is used, since other boreholes are too distant and signals reaching them are considerably attenuated. The treatment may be performed in a vertical or a

*E-mail: bulant@seis.karlov.mff.cuni.cz

horizontal well, while the monitoring is commonly performed in a vertical section of a monitoring well. When the monitoring or the treatment wells are assumed to be vertical, often no borehole deviation survey (i.e., the measurements of the borehole inclination and azimuth, which are then used to calculate the borehole trajectory) is done and the wells are then treated as perfectly vertical. Commonly, orientation of the monitoring geophones is determined from back azimuths of P-waves generated by the perforation shots located in the treatment well, assuming isotropy and lateral homogeneity of the medium between wells. Therefore, the orientation of the geophones in the monitoring well is determined relatively with respect to the position of the treatment well at depths corresponding to the perforations. The orientation (in a geographical coordinate system) of the monitoring array and of the observed microseismic event hypocenters can, however, be obtained only from the positions of the receivers and the perforations. Therefore, any error in the positioning of the monitoring array or of the perforations is directly projected into the error of the fracture-system position. We show that the effects on the fracture-system azimuth may be considerable, even for wells only slightly deviating from their expected positions. Fracture-system geometry (position, azimuth and length) obtained from microseismic monitoring is used, for example, as a guide for an “infill drilling” program, during which new wells are drilled into unfractured (and hopefully undrained) parts of the reservoir. Wrongly estimated fracture azimuth and fracture position may lead to financial losses and an uneconomical infill drilling program.

Additionally, the borehole deviations affect not only the determination of the fracture azimuth, but also the distance between the treatment and monitoring wells. Typically, the initial isotropic velocity model is built from sonic logs and/or vertical seismic profiling (VSP) data in microseismic fracture monitoring. Commonly, the velocity model is then adjusted to locate perforation shots to their assumedly correct positions (Maxwell, Shemeta and House 2006). The velocity model adjustment can be realized in a number of ways but it usually involves fitting S-P-wave traveltime differences. The S-P-wave traveltime differences that cannot be explained by an isotropic model are then fitted by a VTI (transverse isotropy with vertical axis of symmetry) velocity model. We show that such a procedure may lead to a quite strong artificial anisotropy. The artificial anisotropy will cause distorted locations of the microseismic events and thus will distort the shape of the observed hydraulic fracture.

To assess the effects of the borehole deviation uncertainties on fracture azimuth and anisotropic model building, we start

by estimation of the borehole deviation uncertainty from several nearly vertical boreholes. We then show how the borehole deviation uncertainty relates to fracture azimuth and anisotropic model building. Finally, we discuss the relation of the borehole deviation uncertainty and the fracture azimuth uncertainty for an assumed statistical distribution of the borehole deviations.

Throughout the paper, we focus on the case of a vertical monitoring array and a single perforation position. In our illustrative figures we assume the case of two nearly vertical wells, but the results concerning the horizontal uncertainties would also be the same for the case of perforation in a horizontal treatment well. The effects caused by the vertical uncertainties are not studied in this paper. Our results apply to deep as well as shallow boreholes.

BOREHOLE DEVIATION UNCERTAINTIES

Drillers often quote the angular deviation accuracy of an average “vertical” borehole as being 5° . One of the “vertical” wells in a recent monitoring campaign shown in Fig. 1 deviated at the measured (treatment) depth of 1500 m by more than 8° . Figure 1 also shows six other wells in which microseismic monitoring took place and for which deviation surveys were performed. For these wells, the deviation values are mostly within 2° . In the following, we shall thus consider the value of the deviation uncertainty of “vertical” wells with no deviation survey to be 2° , which seems to be a conservative estimate. Note that, with exception of two wells shown in pink and violet in Fig. 1, azimuths of the wells are uncorrelated, i.e., boreholes do not generally deviate in the same direction.

To assess uncertainty in deviation survey measurements, we compared two deviation surveys carried out by two different companies for the same well, and found out that the average difference between the two independent measurements of the borehole deviation was 0.18° . High-quality deviation surveys claim even higher accuracy. To be conservative, and to take into account a systematic error (see, e.g., Williamson 2000), we consider the value of deviation uncertainty of wells with a deviation survey to be 0.5° .

For nearly vertical wells, the deviation uncertainties result mainly in horizontal uncertainty of the positions of the perforations or of the geophones. For simplicity, the vertical uncertainty in their positions will be neglected throughout this paper. Assuming an average deviation uncertainty ω of a nearly vertical well, the horizontal uncertainty y of the well at a measured depth (cable length) h is then $y = h \tan(\omega)$. Considering a typical depth of hydrofracture experiments to be around

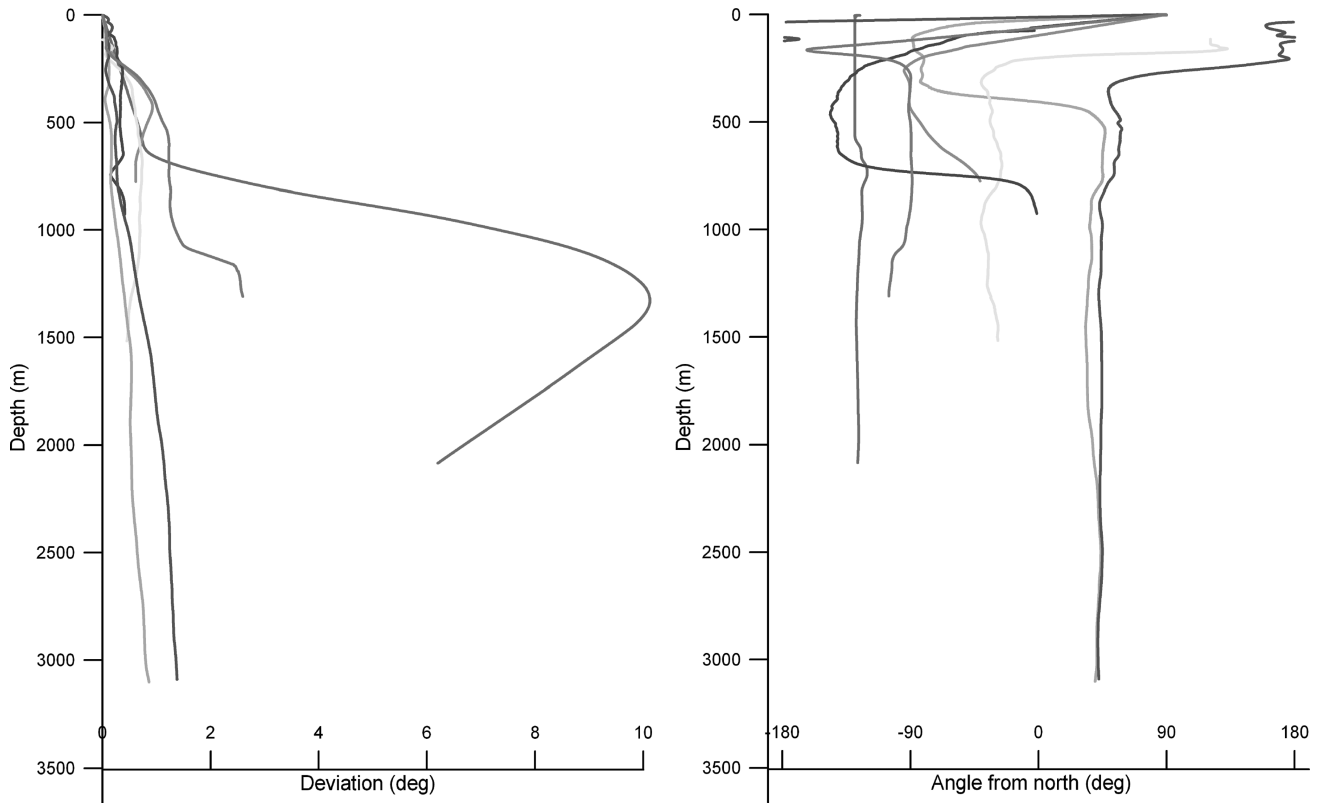


Figure 1 Deviations of seven real wells, where microseismic monitoring of hydraulic fracturing took place, and for which the deviation surveys are available. Left plot shows deviations from vertical, right plot shows azimuths of these deviations. Note that the deviation is unpredictable and may change rapidly in a very short depth range.

Table 1 Horizontal uncertainty, $y = b \tan(\omega)$, at depth b caused by the well deviation uncertainty ω

Depth b (m)	Well deviation uncertainty ω (deg)			
	5	2	0.5	0.2
Horizontal uncertainty $y = b \tan(\omega)$ (m)				
500	43.74	17.46	4.36	1.75
1000	87.49	34.92	8.73	3.49
1500	131.23	52.38	13.09	5.24
2000	174.98	69.84	17.45	6.98
2500	218.72	87.30	21.82	8.73

2000 m, we arrive at a horizontal uncertainty of about 70 m for wells with no deviation survey ($\omega = 2^\circ$), and about 17 m for wells with a deviation survey ($\omega = 0.5^\circ$). For other examples, refer to Table 1. The horizontal uncertainty y has a cumulative effect with measured depth. For shallower depths the uncertainty y is smaller, for greater depths it is larger.

Eisner and Bulant (2006) and Bulant *et al.* (2006) show the effects of neglecting deviation surveys for particular choices of the borehole deviation uncertainty and measured depths. In this study we generalize their specific choices (suitable for direct applications in engineering) and display the resulting fracture azimuth uncertainty and apparent anisotropy as functions of the ratio of the horizontal uncertainty y and the assumed horizontal distance H of the wells, or as a ratio of the true horizontal distance x and the assumed horizontal distance H . As the typical values of H for microseismic monitoring experiments are between 100 and 500 m, we consider the values of y/H to be between 0 and 0.5 (for values of y see Table 1), and the values of x/H to be between 0 and 2, respectively.

FRACTURE AZIMUTH

Let us first examine the effect of the borehole deviation on the fracture azimuth. As described in the Introduction, the fracture azimuth Φ_0 is determined relatively with respect to the assumed positions of the perforation and of the monitoring

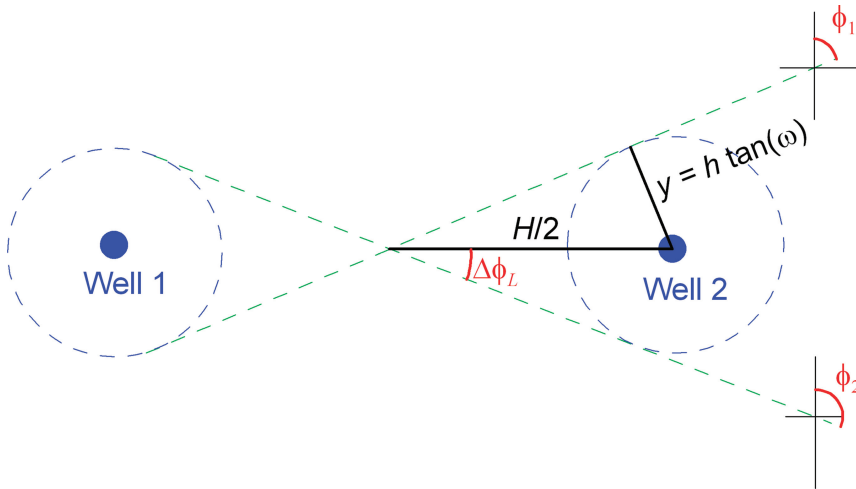


Figure 2 Plan view of a vertical monitoring array (“Well 1”) and a perforation (“Well 2”). The blue dashed circles around “Well 1” and “Well 2” denote maximum deviations from points “Well 1” and “Well 2” in the horizontal plane, respectively. Two green dashed lines tangent to these circles show limiting back azimuths Φ_1 and Φ_2 of a perforation with respect to the monitoring array. $\Delta\Phi_L$ is the maximum fracture azimuth error due to the uncertainty in the positioning of the monitoring array and of the perforation.

array, and any error in the positioning of the monitoring array or of the perforation causes the fracture azimuth error $\Delta\Phi$. The actual fracture azimuth Φ in a geographical coordinate system is thus given as $\Phi = \Phi_0 + \Phi_{SR} \pm \Delta\Phi$, where Φ_{SR} is the azimuth of the perforation-to-receiver direction.

We assume that the monitoring array is vertical. Figure 2 shows a sketch of a plan view of a hydraulic fracture monitoring. The blue point “Well 1” denotes the assumed position of a monitoring array and the other blue point “Well 2” denotes the assumed position of the perforation. H is the horizontal distance between these points. For simplicity, we assume that both wells have the same average deviation uncertainty ω along the entire borehole, and that the perforation and receivers are situated at measured depth b . Generalization of the estimates of the fracture-azimuth error for the case of two different average deviation uncertainties is straightforward.

The blue dashed circles in Fig. 2 show the representative uncertainty of the horizontal positions of the perforation and receivers at the depth b . The two green dashed lines show the limits of the relative back azimuths of the perforation with respect to the monitoring array. The uncertainty $\Delta\Phi$ in the back azimuths of the perforation causes the fracture azimuth uncertainty $\Delta\Phi$, no matter what the angle between the fracture and the source-receiver direction is, i.e., regardless of the relative fracture azimuth Φ_0 . If the borehole trajectories are limited by the deviation uncertainty ω (dashed blue circles in Fig. 2), then the uncertainty $\Delta\Phi$ is limited by the value of $\Delta\Phi_L$, $|\Delta\Phi| \leq |\Delta\Phi_L|$.

We shall now evaluate the uncertainty $\Delta\Phi_L$ in the back azimuth of the fracture for the two limiting cases of the back azimuths shown by dashed green lines in Fig. 2. The relation between this uncertainty and the uncertainty for an assumed

statistical distribution of perforation and monitoring array positions can be found in the Discussion. The simple geometrical sketch shown in Fig. 2 allows us to estimate the nonlinear dependency of the fracture azimuth uncertainty

$$\Delta\Phi_L = \arcsin\left(\frac{b \tan(\omega)}{H/2}\right) = \arcsin\left(2 \frac{y}{H}\right). \quad (1)$$

Figure 3 illustrates the fracture azimuth uncertainty (1) as a function of y/H . Note, that the fracture azimuth uncertainty can be more than 20° for an average deviation uncertainty of 2° at measured depths below 1500 m and a wellhead separation of less than 300 m. This is a common scenario for current microseismic monitoring campaigns in North America. See Table 1, where $\omega = 2^\circ$ and $b = 1500$ m yield $y \sim 50$ m and $y/H \sim 0.17$. Such uncertainty severely limits the use of the fracture geometry for infill drilling decisions. On the other hand, if the average deviation uncertainty ω in the deviation survey is only 0.5° , the ratio y/H is less than 0.074 for $H \geq 300$ m for all depths listed in Table 1. Thus the fracture azimuth is well constrained to less than 7.5° , which is a value rarely achieved from locations of microseismic events. Note that for the values of y/H between 0 and 0.3 the fracture azimuth uncertainty varies approximately linearly, yielding about 11.5° for each 10% increase of y with respect to H . For y/H higher than 0.5, i.e., for possibly crossed borehole trajectories, the fracture azimuth uncertainty is always more than 90° , the fracture azimuth is thus completely undeterminable. Let us also mention that the fracture azimuth uncertainty does not influence the relative locations between individual microearthquakes (the shape of the fracture) but it influences the absolute position and orientation of the fracture as shown in Fig. 5 of Bulant *et al.* (2006).

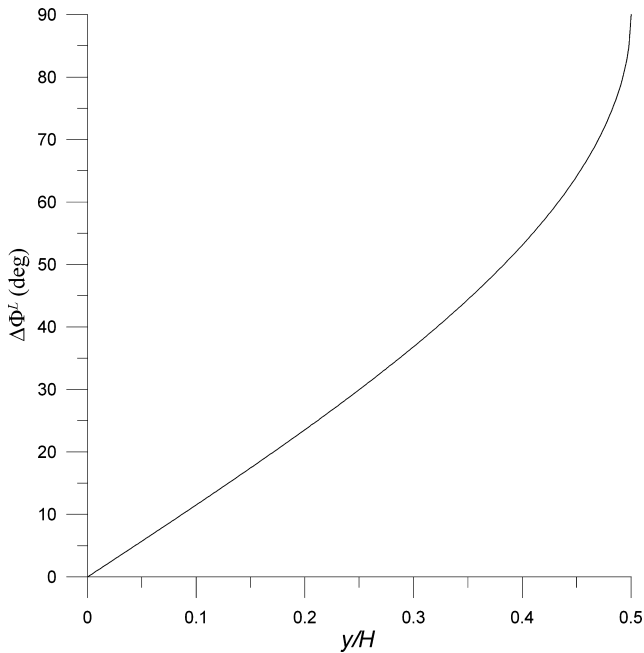


Figure 3 The fracture azimuth uncertainty $\Delta\Phi_L$ in degrees as a function of the ratio of the horizontal uncertainty y and the horizontal distance of wellheads H . For the values of y/H between 0 and 0.3 the fracture azimuth uncertainty is approximately linear, yielding about 11.5° for each 10% increase of y with respect to H . For y/H higher than 0.5, the fracture azimuth uncertainty always exceeds 90° .

APPARENT ANISOTROPY

As explained in the Introduction, it is common to adjust the starting velocity model, obtained from sonic logs and/or VSP, in such a way that the adjusted model yields observed SH-P traveltime differences for the assumed positions of perforations. This is often done by using a VTI model, where vertical velocities match velocities from sonic logs or VSP, and horizontal velocities match the observed SH-P perforation traveltime differences (or P, SH, SV traveltimes if the origin times of perforations are known, Maxwell *et al.* 2006). Such velocity model adjustments are affected by the accuracy of the monitoring and perforation geometry.

To estimate the effects of incorrect perforation-receiver geometry on velocity model adjustment, we numerically analyze a simple example. Let us consider two almost vertical wells deviating from the vertical by an average deviation ω (dashed lines in Fig. 4), and let us investigate traveltime errors caused by treating the wells as perfectly vertical (solid lines in Fig. 4). Let us try to explain the traveltime errors of SH-P by assuming that the homogeneous medium surrounding the boreholes is not isotropic, but a weakly VTI medium. Note that an aver-

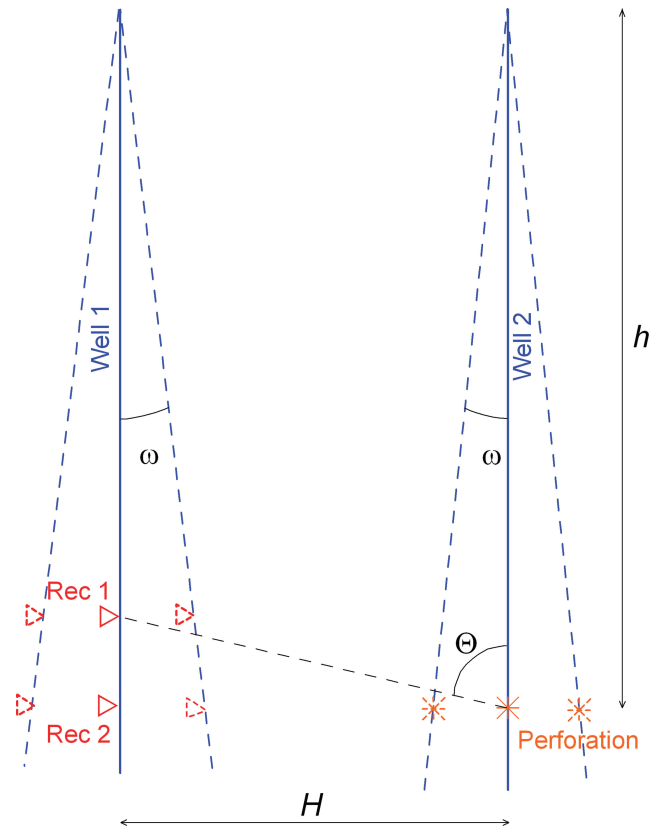


Figure 4 A schematic side-view of two nearly vertical wells (dashed lines) with an average deviation ω from their assumed vertical position (solid lines). H is the assumed horizontal distance of perforation and receiver.

age uncertainty of the well deviation is considered in Fig. 4. Examples of real deviations are shown in Fig. 1.

The difference in traveltimes between true and assumed well positions in a homogenous isotropic medium can be deduced from Fig. 4:

$$\Delta T_{SH-P}(\Theta) = \left(\frac{1}{v_{SH}} - \frac{1}{v_P} \right) \left(\sqrt{\cos^2 \Theta + \frac{x^2}{H^2} \sin^2 \Theta} \right) \frac{H}{\sin \Theta} \quad (2)$$

Here x is the true horizontal distance, while H is the assumed horizontal distance of perforation to receiver array illustrated in Fig. 4. Θ is an angle between vertical and perforation-receiver direction shown by the dashed line in Fig. 4, $\Theta = 90^\circ$ thus corresponds to horizontal propagation. We do not consider the vertical shift of the perforation and of the receiver, since it is negligible in the case of vertical wells; see the Discussion for more details. v_P and v_{SH} are P- and SH-wave velocities. For a given uncertainty of the horizontal well positions (e.g., values y in Table 1), we can estimate $H-2y < x < H+2y$; see Fig. 4. The analysis for an assumed statistical distribution

of perforation and monitoring array positions is detailed in the Discussion.

The traveltime difference (2) can be explained as an effect of a homogeneous weakly VTI medium. P- and SH-wave phase velocities in a weakly VTI medium are given by the following approximate (first-order with respect to the deviations of the VTI medium from isotropic one) formulae:

$$\begin{aligned}\bar{v}_P(\Theta) &= v_P[1 + \delta \sin^2 \Theta + (\varepsilon - \delta) \sin^4 \Theta], \\ \bar{v}_{SH}(\Theta) &= v_{SH}[1 + \gamma \sin^2 \Theta].\end{aligned}\quad (3)$$

Equations (3) are equivalent to equations (16a) and (16c) of Thomsen (1986), respectively. In (3), ε , δ and γ are linearized dimensionless Thomsen's parameters, $\varepsilon = (A_{11} - v_P^2)/(2v_P^2)$, $\delta = (A_{13} + 2A_{55} - v_P^2)/v_P^2$, and $\gamma = (A_{66} - v_{SH}^2)/v_{SH}^2$, A_{ij} denoting density-normalized elastic moduli in the Voigt notation. The parameters ε , δ , and γ together with v_P and v_{SH} specify the VTI medium. The parameters ε , δ , and γ characterize deviations of a weakly VTI medium from an isotropic one. If multiplied by 100%, ε and γ can be used to estimate the strength of P- and SH-wave anisotropy in %, respectively, δ controls curvature of the P-wave phase-velocity surface around the axis of symmetry (Tsvankin 2001). v_P and v_{SH} represent vertical P- and SH-wave phase velocities, respectively. The first-order (linearized) P- and SH-wave traveltimes T_P and T_{SH} , respectively, between perforation and receiver can be determined from Eqs. (3):

$$\begin{aligned}T_P(\Theta) &= \frac{1}{v_P} [1 - \delta \sin^2 \Theta - (\varepsilon - \delta) \sin^4 \Theta] \frac{H}{\sin \Theta}, \\ T_{SH}(\Theta) &= \frac{1}{v_{SH}} [1 - \gamma \sin^2 \Theta] \frac{H}{\sin \Theta}.\end{aligned}\quad (4)$$

Traveltime difference ΔT_{SH-P} of the SH- and P-wave in a homogeneous weakly VTI medium then reads

$$\begin{aligned}\Delta T_{SH-P}(\Theta) &= \left[\left(\frac{1}{v_{SH}} - \frac{1}{v_P} \right) - \left(\frac{1}{v_{SH}} \gamma - \frac{1}{v_P} \delta \right) \sin^2 \Theta \right. \\ &\quad \left. + \frac{1}{v_P} (\varepsilon - \delta) \sin^4 \Theta \right] \frac{H}{\sin \Theta}.\end{aligned}\quad (5)$$

Equation (5) does not allow independent determination of all 3 parameters of the VTI medium (γ , δ , and ε) as there are only two terms of angular dependency of the traveltime difference. Thus we introduce two coefficients, G and E :

$$G = \gamma - \frac{v_{SH}}{v_P} \delta \quad \text{and} \quad E = (\varepsilon - \delta),\quad (6)$$

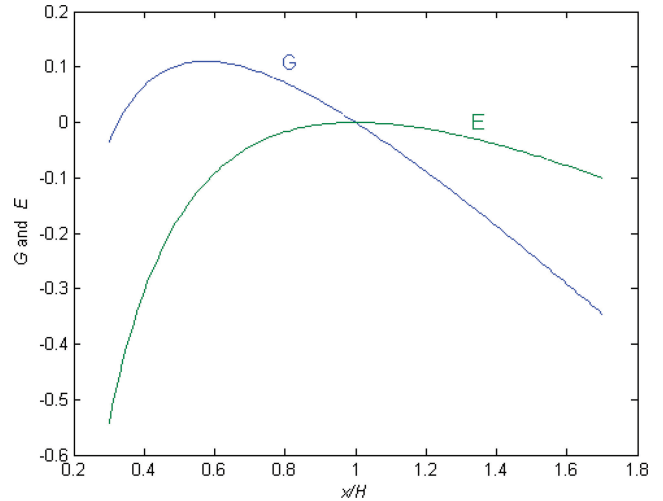


Figure 5 Best fitted VTI anisotropic parameters that would compensate the traveltime difference caused by geometrical error due to unknown deviation survey. The blue and green curves represent two coefficients G and E defined in equation (6). The values of coefficients G and E were obtained by least-square fitting of equation (7) to the traveltime differences calculated from equation (2) at 8 receivers with vertical spacing of 30 m and assumed source-receiver horizontal distance $H = 500$ m in the homogenous isotropic model ($v_P = 4400$ m/s, $v_{SH} = 2600$ m/s). For an example of the traveltime differences compensation, refer to Fig. 6.

and rewrite equation (5) as

$$\Delta T_{SH-P}(\Theta) = \left[\left(\frac{1}{v_{SH}} - \frac{1}{v_P} \right) - \frac{G}{v_{SH}} \sin^2 \Theta + \frac{E}{v_P} \sin^4 \Theta \right] \frac{H}{\sin \Theta}.\quad (7)$$

If the parameter δ is zero, $G = \gamma$ and $E = \varepsilon$.

The traveltime difference (7) can be matched to the traveltime difference due to incorrect geometry in equation (2). Note that the ratio, x/H , of the assumed to the true distance controls the ΔT_{SH-P} delay in equation (2), thus this ratio controls the strength of apparent anisotropy induced by incorrect geometry.

Figure 5 shows results of the least square inversion of equation (7) for traveltime differences computed from equation (2) at 8 receivers (30 m vertical spacing, centered on the depth of the perforation) in a homogeneous isotropic velocity model ($v_P = 4400$ m/s, $v_{SH} = 2600$ m/s). Note that $G = E = 0$ for $x/H = 1$, i.e., if the true and assumed horizontal distances are equal, the inversion yields the true isotropic model. For $x/H > 0.5$ the inversion is not sensitive to a chosen velocity model, assumed distance H , or number of receivers or their spacing. Traveltime differences in equation (2) increase with increasing deviation from 1 of the ratio between the real

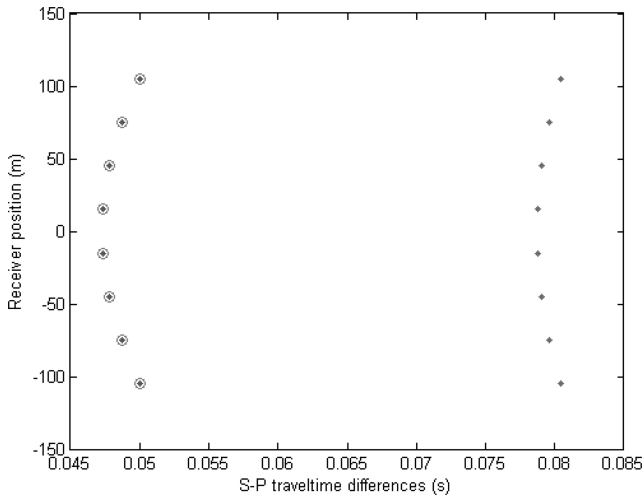


Figure 6 SH-P-wave traveltimes differences computed at 8 receivers in a homogeneous isotropic model used for generation of Fig. 5, for perforations 500 m away (assumed horizontal distance: green dots) and 300 m away (true horizontal distance: blue dots). The red circles represent SH-P traveltimes differences computed at 8 receivers in the homogeneous anisotropic model with $G = 0.11$ and $E = -0.09$ for perforation 500 m away. Note that the values of $G = 0.11$ and $E = -0.09$ correspond to $x/H = 0.6$ from Fig. 5, i.e., to the true horizontal distance 300 m and the assumed horizontal distance 500 m. The anisotropic model perfectly explains the traveltimes discrepancy due to incorrect assumed geometry.

distance x and the assumed distance (wellhead spacing) H . For a fixed wellhead spacing H this ratio increases with measured depth, as the uncertainty in H is linearly proportional to the measured depth (Bulant *et al.* 2006). Note that both G and E are negative if the assumed distance between the perforation and the receivers is shorter than the true distance, i.e., if $x/H > 1$ in equation (2). Let us emphasize that the approximate formulas (3), (4), (5), and (7), used for the estimates of the coefficients (6), work reliably for anisotropy up to approximately 20%. Possible stronger anisotropy resulting from the above formulae thus only indicates strong distortions in the well geometry. Let us also note that if the average deviation uncertainty ω is only 0.5° , i.e., deviation surveys are performed, the ratio x/H is limited in the interval $0.86 < x/H < 1.14$ for $H \geq 300$ m for all depths listed in Table 1. The absolute values of parameters G and E are thus less than 0.07.

Figure 6 shows traveltimes differences between true and assumed geometry in isotropic medium used for generation of Fig. 5, and assumed geometry with the best fitted anisotropic model. Note that the anisotropic model perfectly explains the traveltimes discrepancy due to incorrect assumed geometry.

DISCUSSION

The goal of this article is to present evidence that deviation surveys are important for monitoring induced microseisms generated in relation to hydraulic fracturing treatment. We have analyzed the uncertainty in the fracture azimuth and the possibility of introducing artificial anisotropy due to geometrical effects caused by uncertainty in deviation surveys. However, there are numerous other reasons why accurate deviation surveys are necessary. For example, Fig. 5 of Bulant *et al.* (2006) illustrates that deviation-survey uncertainty is the main cause of uncertainty in the location of microseismic events. Deviation surveys are necessary for velocity model building from multiple sonic log measurements, for geometrical relationship between injection points and fracture, etc.

In this study, we have assumed two nearly vertical wells, both with the same average deviation ω from the vertical causing an uncertainty γ in the horizontal positions of the source and receivers located deep in the boreholes. We then studied the effects of the horizontal uncertainty on the retrieved fracture azimuth, and estimated the 'maximum' fracture azimuth uncertainty $\Delta\Phi_L$ corresponding to the extreme case displayed in Fig. 2. We have shown that in this case every percentage point of the horizontal position uncertainty means approximately 1° uncertainty in the azimuth of the fracture; see Fig. 3.

To evaluate the fracture azimuth uncertainty statistically, we need to assume a statistical distribution of the borehole deviations and a relation between deviations of the two considered wells. The seven borehole trajectories shown in Fig. 1 do not allow such a study. Thus, we assume Gaussian distribution of the horizontal positions of both monitoring array and perforation shot, and mutually uncorrelated deviations of the two wells. Analytical evaluation of standard deviation of back azimuths $\Delta\Phi_S$ requires double-integration of complicated elliptical integrals which, to the best of our knowledge, do not have analytical solutions. For two sufficiently distant wells, i.e., for the case of $\sigma \ll H$, we can use Taylor expansion of $(\Phi)^2$ with respect to Cartesian coordinates of perforation and monitoring array, and the first-order term of the expansion yields $\Delta\Phi_S \approx 1/\sqrt{2} \arcsin(\frac{\sigma}{H/2})$ (L. Klimeš, pers. comm. 2006). Here, σ is the standard deviation of the selected Gaussian distributions for both monitoring and treatment wells. From numerical tests we found that the above approximate relation is sufficiently accurate for $\sigma/H < 0.3$. This means that for $\sigma/H < 0.3$, $\Delta\Phi_S$ as a function of σ/H behaves in the same way as $\Delta\Phi_L$ as a function of γ/H , multiplied by $1/\sqrt{2} \cong 0.7$; see equation (1). Dependence of $\Delta\Phi_S$ on σ/H

can be thus illustrated by the curve in Fig. 3 if we substitute y/H by σ/H and $\Delta\Phi_L$ by $\Delta\Phi_S/0.7$.

Analogously, we could discuss appropriate choice of the parameter x in equation (2) under the assumption of Gaussian distribution of horizontal positions of both monitoring array and perforation shot. The parameter x then would be in an interval $(H - 1.4\sigma, H + 1.4\sigma)$ for $\sigma/H < 0.3$.

In this study we neglected vertical shifts due to uncertainty in the deviation surveys. The reasons to neglect the vertical shifts are twofold. For nearly vertical boreholes,

- the vertical shift due to unknown deviation surveys always reduces the assumed depth, both of the monitoring apparatus as well as the perforation. Thus the corrections in vertical direction for monitoring and treatment wells are correlated.
- the vertical shift is negligible relative to the horizontal ones. For a deviated straight well, the horizontal shift is $b \sin(\omega)$, while the vertical shift is $b [1 - \cos(\omega)]$, where b is the measured depth. For the examples given in Table 1, the vertical shift ranges from 9.5 m to 1 cm while the horizontal shift ranges from 218 to 5 m.

The average uncertainty (deviated straight wells) may slightly underestimate the vertical shift. However, even for the deviations of the real wells (Fig. 1) the horizontal shifts are orders of magnitude larger than the vertical ones. Let us also point out that the vertical shifts do not affect the uncertainty on the azimuth of the fracture. Significant (comparable to the receiver spacing) vertical shifts between perforations and monitoring arrays due to unknown deviation surveys may cause apparent tilted VTI anisotropy.

Without accurate deviation surveys, considerably distorted results can be obtained. Assuming we have not adjusted the velocity model using erroneous geometry, the relative locations among microseismic events do not change (see Fig. 5 of Bulant *et al.* 2006). However, if we adjust the velocity model using erroneous geometry and introduce artificial anisotropy, even the relative locations are distorted. The relative positions of the perforation shots (or injection points) and of microseismic events are in such cases also distorted.

Finally, we would like to mention that in the case of microseismic monitoring in horizontal wells, the presented results should be generalized, especially by including vertical as well as horizontal uncertainty. Horizontal wells are usually longer. Thus, even for a horizontal well with a measured deviation survey, the uncertainty in perforation shot position may be significant. However, the effects of the incorrect position are geometry-dependent and should be evaluated on a case-by-case basis.

CONCLUSIONS

The presented results show that the applicability of the results of monitoring of induced microseisms generated in relation to hydraulic fracturing treatment is severely limited if borehole deviation surveys of treatment or monitoring wells are not performed. Deviation surveys are an important factor affecting the quality of the information that can be obtained from microseismic monitoring of hydraulic fracturing. The importance of the deviation-surveys accuracy increases with the measured length of the wells and with the length of the monitoring array. It also increases as spacing between monitoring and treatment wells decreases. Horizontal uncertainties of receiver or perforation positions need to be considered for microseismic monitoring in vertical wells, and they are also necessary for horizontal wells. For horizontal wells, the vertical uncertainties also play important role. Estimation of the effects caused by the vertical uncertainties may be done following similar steps to those in this study.

Microseismic monitoring with deviation surveys of both monitoring and treatment wells reduces uncertainty in the observed locations of microseismic events and provides accurate and reliable information.

ACKNOWLEDGEMENTS

The authors are grateful to Luděk Klimeš, Chris Chia, Ian Bradford and Scott Leanney for useful and stimulating discussions. We would also like to thank the anonymous reviewer for useful recommendations and the European Union for funding the IMAGES Transfer of Knowledge project (MTKI-CT-2004-517242). This research has been partially supported by the Grant Agency of the Czech Republic under Contract 205/07/0032.

REFERENCES

- Berumen S., Gachuz H., Rodriguez J.M., Lapierre Bovier T. and Kaiser P. 2004. Hydraulic fracture mapping in treated well channelized reservoirs development optimization in Mexico. 66th EAGE meeting, Paris, France, Extended Abstracts, H027.
- Bulant P., Eisner L., Pšenčík I. and Le Calvez J. 2006. Borehole deviation surveys are necessary for hydraulic fracture monitoring. Abstracts of SPE Annual Technical Conference, San Antonio, SPE 102788, Society of Petroleum Engineers.
- Eisner L. and Bulant P. 2006. Borehole deviation surveys are necessary for hydraulic fracture monitoring. 68th EAGE meeting, Vienna, Austria, Extended Abstracts, P305.

- Maxwell S.C., Shemeta J. and House N. 2006. Integrated anisotropic velocity modeling using perforation shots, passive seismic and VSP data. 68th EAGE meeting, Vienna, Austria, Extended Abstracts, A046.
- Rutledge J.T. and Phillips W.S. 2003. Hydraulic stimulation of natural fractures as revealed by induced microearthquakes, Carthage Cotton Valley gas field, east Texas. *Geophysics* **68**, 441–452.
- Thomsen L. 1986. Weak elastic anisotropy. *Geophysics* **51**, 1954–1966.
- Tsvankin I. 2001. *Seismic Signatures and Analysis of Reflection Data in Anisotropic Media*. Elsevier Science.
- Warpinski N.R., Branagan P.T., Peterson R.E., Wolhart S.L. and Uhl J.E. 1998. Mapping hydraulic fracture growth and geometry using microseismic events detected by a wireline retrievable accelerometer array. Abstracts of SPE Gas Technology Symposium, SPE 40014-MS, Society of Petroleum Engineers.
- Williamson H.S. 2000. Accuracy prediction for directional measurement while drilling. *SPE Drilling & Completion* **15**, 221–233.

